We are IntechOpen, the world's leading publisher of Open Access books Built by scientists, for scientists

4,800
Open access books available

122,000
International authors and editors

135M
Downloads

154
Countries delivered to

Our authors are among the

TOP 1%
most cited scientists

12.2%
Contributors from top 500 universities

CLARIVATE ANALYTICS
BOOK CITATION INDEX
INDEXED

WEB OF SCIENCE™

Selection of our books indexed in the Book Citation Index
in Web of Science™ Core Collection (BKCI)

Interested in publishing with us?
Contact book.department@intechopen.com

Numbers displayed above are based on latest data collected.
For more information visit www.intechopen.com

Composition Electrolytic Coatings with Given Functional Properties

Gulmira Yar-Mukhamedova, Maryna Ved',
Nikolay Sakhnenko and Tetiana Nenastina

Abstract

Ternary alloys of cobalt with molybdenum and tungsten deposited from biligand citrate-pyrophosphate electrolyte by pulsed mode exhibit different compositions and surface morphologies depending on current density and on/off time. The structure of binary and ternary alloys was found to be amorphous crystalline, and intermetallic phases Co_7W_6 and Co_7Mo_3 were identified in deposits. The coherent-scattering region size of the amorphous part was detected of 2–8 nm. The amorphous structure of ternary alloys and significant content of alloying elements (Mo and W) predetermine improved high corrosion resistance. Corrosion resistance of binary and ternary deposits increases with total content of refractory metals, which associated with molybdenum and tungsten, enhancing corrosion resistance to pitting as well as decreasing in roughness and smoothing out the relief of ternary coatings. Ternary galvanic alloys of cobalt with molybdenum and zirconium with micro-globular morphology with low level of stress and cracks are formed at a current density of 4–6 A dm^{-2} and polarization on/off time 2/10 ms. High corrosion resistance of ternary coatings based on cobalt is caused by the increased tendency to passivity and high resistance to pitting corrosion in the presence of molybdenum and zirconium, as well as the acid nature of their oxides.

Keywords: coating, electrodeposition, composition, physicomechanical properties

1. Introduction

The range of functional coatings with alloys, the creation of which to a large extent predetermined the progress of modern technologies, can be fully attributed to the advances of electrochemical science. Quite obvious consumer advantages of coatings with alloys, in comparison with monometallic analogues, led to prospects for their widespread use, despite a number of technical difficulties encountered. The twenty-first century brought new challenges—amorphous alloys, nanoscale, nanocrystalline, and nanolaminate structures, film materials with gigantic magnetic resistance or high-temperature superconductivity, multiferroics, etc., became the order of the times, the formation of which on the basis of trivial bimetallic compositions proved impossible. This led to the creation of a new paradigm in practical electroplating—the only alternative to the transition to multicomponent and synergistic alloys and composites. The implementation of it put a number of pressing problems in the design of such polymetallic systems.

The essence of the problem lies in the absence of clear design algorithms for multicomponent alloys with a given level of properties and the presence of a significant number of empirical views, the use of which allowed electrochemical gurus to bypass the obstacles of Mother Nature in creating electroplated coatings with alloys. New tasks required new approaches, but before proceeding to their consideration, let us analyze the essence of the problem in the formulation "Galvanic alloys—the philosophy of synergism".

1.1 Alloys

The physical encyclopedia gives the classical definition of an alloy as "a metallic, macroscopically homogeneous system consisting of two or more metals (less commonly metals and nonmetals) with characteristic metallic properties." The etymology associates the material with the method of its preparation—the combination of individual components during melting followed by crystallization of the melt, although dozens of other methods are currently known. In addition, the definition of "macroscopically homogeneous" raises the question of whether heterogeneous structures (mechanical mixtures) belong to the alloy community. Apparently, it is more correct to speak of metal alloys as homogeneous or heterogeneous systems, as well as intermetallic compounds, although it is quite obvious that real alloys often contain all three types of these structures. Regarding the "metallic properties," we note that a wide class of compounds—"synthetic metals" [1, 2]—has all the above features (hardness, electrical and thermal conductivity, opacity, gloss, etc.), but does not contain metals at all, if you do not take attention cations.

1.2 Galvanic alloys

In this formulation, the nature of the material and the method of its production are inextricably linked, but with all the apparent uniqueness, and there is a number of significant differences not only in the structure and properties of metallurgical and galvanic alloys but also in the concentration ratios of the components in the material. During electrolytic deposition, alloys can be formed that differ essentially in their phase composition and properties from those obtained by thermal means. This expands the range of technical capabilities of electrolytic alloys and their field of application.

1.3 Synergism

The term "synergetic" means joint or corporate action, and the synergistic effect is an increase in the efficiency of activity as a result of integration, the merging of separate parts into a single system. The question is to what extent the terminology of synergetic, or rather, actually synergism, is applicable to such objects as electrolytic alloys? From the definition of the object of research of synergetic "processes in complex open non-equilibrium systems …" [3], it follows that the combination of these system-forming features is fully applicable to process in electrochemical systems, which include alloy formation. Indeed, such an electrochemical system is complex, open, and nonequilibrium under the conditions of application external polarization.

For example, the advantage of coatings with alloys in comparison with individual metals, as well as the realization of synergism during the electrolytic alloy formation, manifests themselves in a change in the microhardness of materials depending on their composition and structure (**Table 1**). It is obvious that the formation of intermetallic compounds in the systems "metal of the iron

family—molybdenum or tungsten," as well as the formation of amorphous structures, creates the prerequisites for a super-additive increase in the microhardness of the coatings.

Among the methods for solving complex technical problems, we will highlight both a deep understanding of the problem by creating a formalized description based on a systematic approach, followed by analysis and synthesis of complex systems, and a black box principle that does not involve a combination of the above actions, but is no less effective when using artificial intelligence tools, for example, artificial neural networks [9]. It is clear that the most significant results can be achieved with the integrated use of both approaches. In the first case, the electrochemical system (ECS), as a complex object in which the phenomena of substance transfer and electrical and thermal energy are realized, is characterized by a set of input and output variables, a set of parameters of electrode reactions and related physic-chemical transformations.

Since all components of the system are in constant development, they should be considered as processes, extending this procedure to subsystems. Therefore, to describe ECS in the field of external disturbances, it is necessary to identify the elements and links that make up the system and to establish the interaction between them, thus linking the functions and structures [10]. The set of processes in ECS can be represented as the implementation of transformations in the intersection of the subsets: ionic medium (electrolyte), electrode (electrode material), external disturbances (individual factors, as well as their joint or complex effect), as we have previously shown in the framework of corrosion protection analysis [11].

Among the most significant external influences, it is necessary to attribute, mainly, the different nature of the field (vector quantities), among which are:

- an electric field (polarization), including nonstationary modes of electrolysis with varying amplitude and temporal characteristics;

- a temperature field, which allows control not only the temperature of the reaction volume but also the aggregation state of individual elements (solutions-melts-gas phase), while the rate of change $\Delta T/\Delta t$ allows you to control the transformation routes (for example, supersaturation of solutions, the formation of 2- and 3-dimensional nuclei, the formation of amorphous structures, etc.);

- a magnetic field (factor in electrochemical processes is nonexhaustible, but the studied is completely insufficient),

- a pressure (creation of excessive pressure or vacuum);

| Monometallic coatings	H_V	Intermetallic compounds and alloys	H_V
Cr (lustrous) [4]	7.5–11.0	CoW [6]	8.3
Cr (milk) [4]	4.5–6.0	Co_3W [6]	5.1
Cr (from tetrachromat bath) [4]	3.5–4.0	Co—W [5]	3–6.8
Co [5]	1.6	Fe—W [7]	13
Fe [5]	4.5–7	Ni—W [5]	2–14
W (from melt) [6]	3.7	Fe—W—P [8]	≥11

Table 1.
Microhardness (GPa) by Vickers galvanic coatings of metals and metal alloys.

- an impulse of movement, including the ultrasound field (mixing, transfer of reactants, or electrolysis products);

- a radiation (radiation field), which, depending on the nature, can lead, for example, to radiolysis, change of electrolysis conditions under the action of laser irradiation or structure and surface properties of the electrode material, as well as other changes in the state and properties of individual phases and even transformation routes;

- a gravitational field, which changes the conditions for the electrochemical processing (e.g., the stages of transportation), as well as other, less significant effects.

As an example, one can analyze the contribution of individual groups of process parameters (**Figure 1**) to the formation of synergistic alloys [12]. Thus, varying the composition of the electrolyte, the modes and parameters of the electrolysis, we electroplated iron alloys with refractory metals of different compositions and morphologies [13–15], which determine the level of functional properties (**Figure 2**).

Cobalt-based alloys are widely used as construction materials for different technic applications, for example, super alloys for aircraft turbine vanes and blades, alloys for powerful, high-coercive force magnets, hard metal alloys for cutting tool materials, and protective hard coatings. Cobalt is utilized as a matrix of special materials, including alloys for dental and surgical implants or bone fracture fixation, thermal resistant materials (Fe—Ni—Co, Co—Fe—Cr), magnetic recording thin films, catalysts [16], etc.

The addition of refractory metals (molybdenum, tungsten, zirconium, etc.) even in small amounts to cobalt significantly extends the functional properties of materials. In some cases, of particular interest is the implementing of these properties in thin surface layers. High adhesion and a wide range of coating composition are provided by electrodeposition from aqueous and nonaqueous solutions.
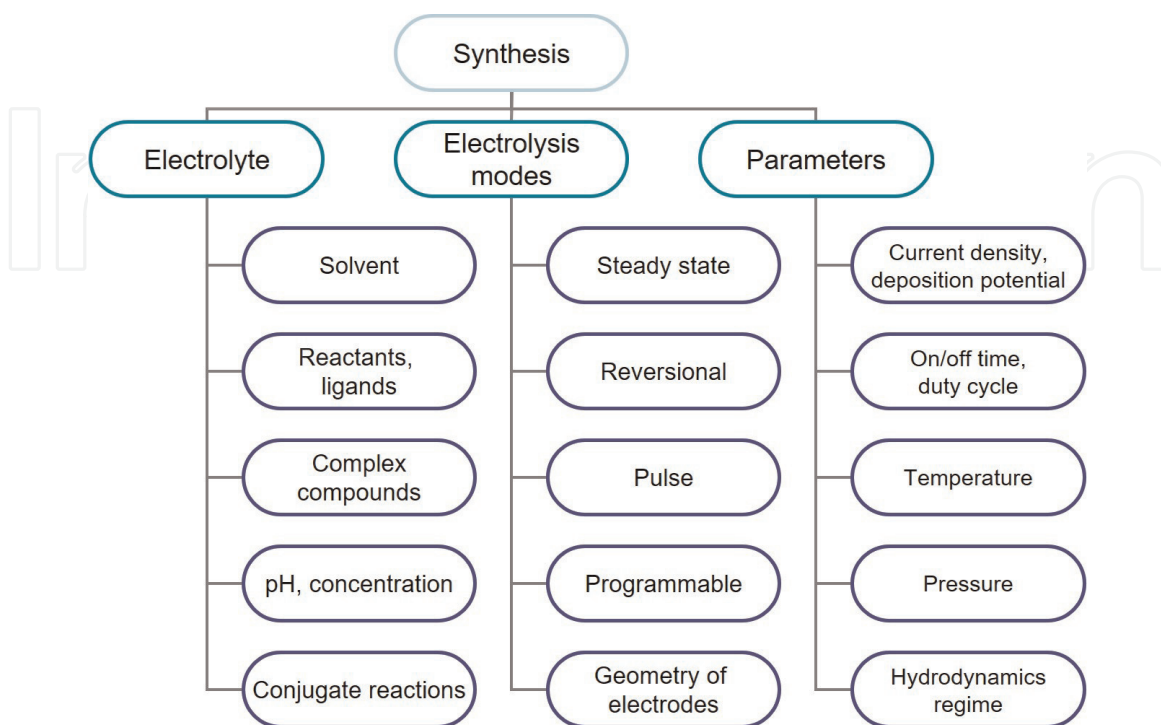
Figure 1.
The main factors of electrolytic alloying.
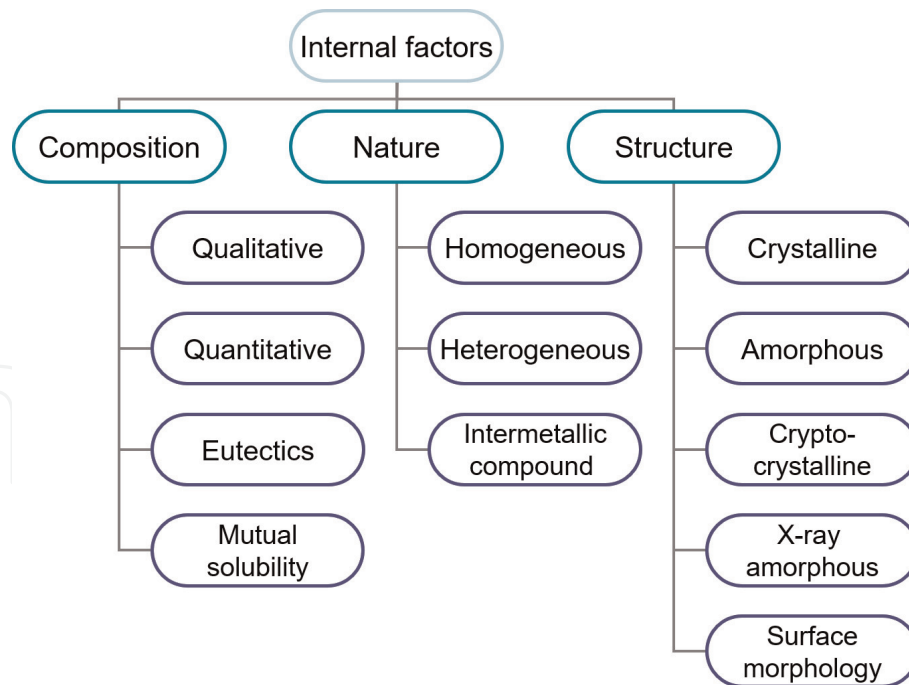
Figure 2.
Internal factors forming the functional properties of the alloys.

Electrodeposition peculiarities of binary and ternary cobalt alloys with molybdenum as well as their properties are reflected in promising publications. Cobalt-molybdenum (ω_W is 10%) films with low coercivity and high saturation magnetization were formed from a sulfate-citrate bath [17]. It was shown that the dependence of electrolytic alloy structure on the current density, namely a close-packed hexagonal structure, was formed at low cathodic polarization, and both crystalline and amorphous structures were appeared at higher polarization [18]. High adherent, compact, and uniform cobalt and cobalt-molybdenum coatings with 1–8 wt. % Mo were deposited onto copper substrates from ionic liquids based on choline chloride (ChCl) at a current density of 7–25 mA cm^{-2}, at 90–100°C [19]. Cobalt-molybdenum-boron amorphous electrolytic alloys of composition, wt. %: Co—51, Mo—47, and B—2, were deposited from citrate-phosphate-ammonia bath at a cathode current efficiency of 29–65%. Above materials exhibit high hardness, corrosion resistance, wear resistance, and also sufficient ductility [20]. Cobalt-molybdenum-phosphorus (Co—Mo—P) coatings containing 8% Mo, 20% P, and Co balance were deposited from citrate-phosphate electrolyte and were recommended as barrier layer to replace nickel [21]. The amorphous Co—Mo—C coatings were deposited with additional exposure of working electrode in the magnetic field. The content of Mo in the coatings deposited in a magnetic field increases up to 34.2 at. % as compared with traditionally deposited alloys [22]. A growth of overvoltage during hydrogen evolution at above materials was also observed.

Thus, in particular, the light lustrous uniform coatings made of iron binary and ternary alloys with refractory metals were deposited from complex electrolytes both at direct and pulse current. It was noted fairly high deposition rate up to 20 μm/h and the current efficiency of 60–85%, which is much higher as compared with the results of other scientists [23–25]. The morphology and topography of the coatings were shown to be depended on the nature of alloying refractory metals and the electrolysis modes on the course of the electrochemical alloy forming reactions. The reason was the change in the nature of the discharging particles and the limiting stage of the net electrode process.

The biligand citrate-pyrophosphate electrolyte [26, 27] was used for codeposition cobalt with molybdenum and tungsten to overcome significant potential difference of alloying metals which also are reduced multistage [12, 13]. The binary Co—Mo [26] and Co—W [5] deposits were obtained, and their composition was controlled by the variation of the pH and the concentration ratio of alloying metals' and ligands in a bath. The formation of hetero-nuclear complexes cobalt, molybdate, and tungstate with citrate and pyrophosphate, and complexes subsequently reducing into an alloy, may be competing with each other as it was shown for iron ternary [28, 29], Co—Mo—Zr [30] and Co—Mo—W deposits.

Ternary Co—Mo—Zr alloys were also deposited from citrate-pyrophosphate electrolyte with optimal concentration ratio of molybdate and tungstate for ligands [30, 31]. It was shown the advantage to use electrolyte with tungstate excess compared with molybdate. In addition, the use of pulse current was contributing to the deposition of ternary alloys with a high content of refractory metals.

2. Co—Mo—W electrolytic alloys

Figure 3 shows the current efficiency and composition of deposits Co—Mo—W plated from bi-ligand (citrate-pyrophosphate) bath in pulse regime at ratio $t_{on}/t_{off} = 5/20$ ms. The total deposition time is 30 min. As we can see from the plots, the total alloying metal content in the deposits Co—Mo—W rises from 19 at. % up to 30 at. % with increasing cathodic polarization from 4 to 10 A dm^{-2}. This phenomenon is quite natural and is due to the shift of the electrode potential in the site of oxometalates reducing with increasing current density. The decrease in the alloying metal content with an increase in the current density of more than 10 A dm^{-2} is associated with the intensification of the side reaction of hydrogen evolution. The current efficiency decreases with current density also due to the impact of the side reaction of hydrogen evolution. Indirectly, a decrease in the current efficiency with an increase in the refractory metal content may be due to the alloy catalytic activity in the electrolytic hydrogen evolution.

Both the morphology and composition of ternary alloys deposited in pulse mode at current density 8 A dm^{-2}, on/off time 5/20 ms depend on the electrolyte temperature (**Figure 4**). Since it was established earlier that lower current densities 5–7 A dm^{-2} favor higher current efficiency, this growth is due to the formation of
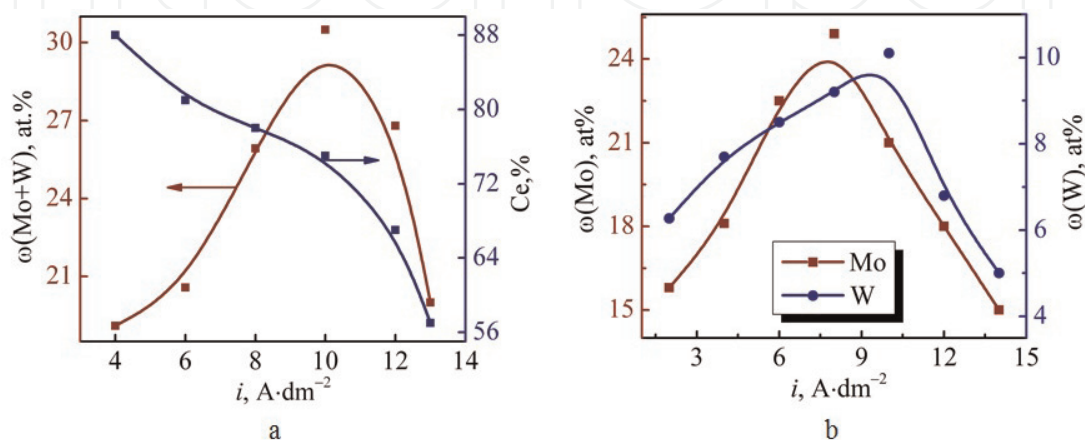
Figure 3.
Dependence of current efficiency Ce, total refractory metal content (a), and Mo or W content (b) in Co—Mo—W alloy on applied current density.
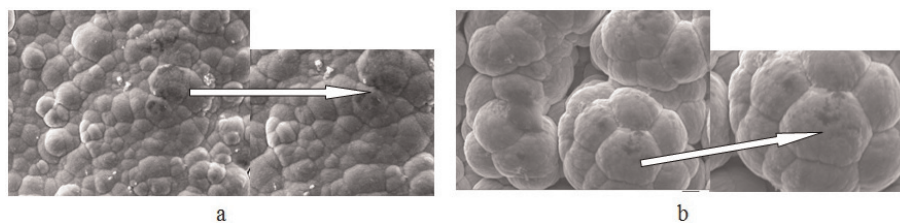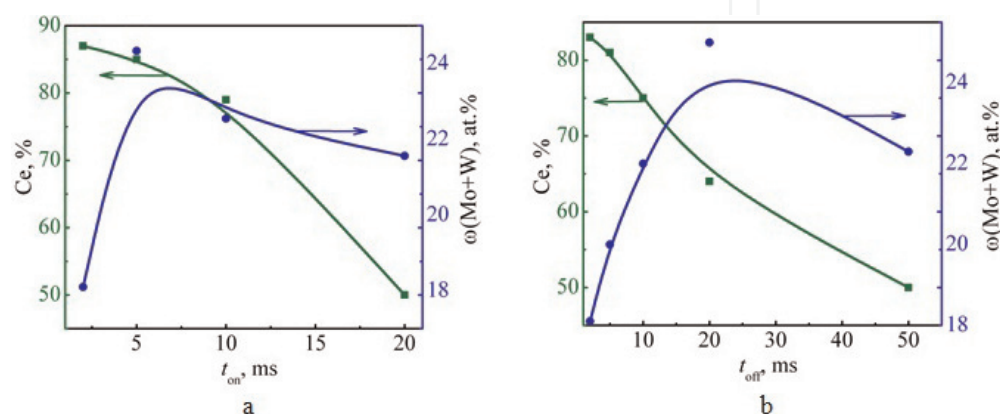
Figure 4.
Morphology and refractory metal content (at. % in terms of metal) in Co—Mo—W coatings, deposited at:
(a) T = 30°C, Co—86.6, Mo—7.0, W—6.4; (b) T = 50°C, Co—83.2, Mo—10.7, W—6.1. Magnification
×2000/5000.

intermediate molybdenum and tungsten oxides instead of metals as suggested by the appearance of the deposited coatings. Those plated using current densities 8 A dm^{-2} are smooth, compact, and microglobular. Those obtained using higher temperature of 50°C (**Figure 4b**) have developed globular surface with larger sizes of agglomerates and microspheroids. With an increase in the temperature, the relative content of molybdenum also increases, and tungsten one changes slightly. Despite WO_4^{2-} : MoO_4^{2-} ratio in the electrolyte of 1:2, the coatings are enriched with molybdenum.

It is obviously molybdenum and tungsten compete with each other during deposition into an alloy, and therefore the atomic ratio of metals in the coating differs from the ratio of oxoanion concentrations in the electrolyte [30]. In turn, the atomic ratio of metals in the alloy determines the structure of the morphology of the surface layers. So, it is the increase in $\omega(W)$ that causes deep microcracks in the coating to a greater extent than the growth of the total refractory metal content [33].

Time parameters of pulsed electrolysis namely on/off time impact the current efficiency and composition of ternary alloys (**Figure 5**). Increasing the polarization time within the range of 2–5 ms at the current density of 10 A dm^{-2} and pause time 20 ms promotes content, both refractory components, in the coating (**Figure 5a**) but more significantly for tungsten. No any significant change in refractory metal content observed at longer polarization. As it follows from experiment (**Figure 5b**), the optimal off-time for alloying metal content is in the range of 15–20 ms when on-time is 5 ms. Thus, we can conclude that the pulse/pause ratio of 1/ (3–4) provides the maximum content of molybdenum and tungsten in the alloy. Considering the molybdenum competition with tungsten when forming hetero-nuclear complexes discharged at the cathode, the energy and time parameters of electrolysis despite

Figure 5.
Dependence of refractory metal content and current efficiency for Co—Mo—W alloys deposited from bi-ligand bath on parameters of pulse electrolysis: on-time (a) at t_{off} = 20 ms and off-time (b) at t_{on} = 5 ms.

the ratio of the molybdate and tungstate concentrations in a solution are the tools for ternary alloy composition control.

Current efficiency decreases in the range of 87–52% when increasing on-time is caused by the hydrogen evolution enhancement (**Figure 5a**). Prolong the pause as compared with pulse time positively influences the current efficiency as subsequent chemical reactions accompanying the alloying metals discharge are more fully. A larger current interruption than for 20 ms reduces the efficiency of the process (**Figure 5b**) as it was also observed in [34]. Thus, high refractory metal content in the Co—Mo—W alloy while maintaining a reasonable value of current efficiency Ce 70–75% at a current density of 10 A dm^{-2} is achieved with t_{on}/t_{off} = 5/20 ms.

Figure 6 shows X-ray diffraction patterns for Co—Mo—W alloys deposited on a copper substrate at a pulse current amplitude of 8 A dm^{-2}; t_{on}/t_{off} = 2/10 ms (**Figure 6**, black line) and a direct current density of 4 A dm^{-2} (**Figure 6**, red line); T = 30°C; coating thickness is 20 μm.

The X-ray diffraction patterns indicate an amorphous-crystalline structure of the alloys. The high intensity peaks at 60 and 90° are copper substrate lines. We can see some peaks corresponding to α-Co phase, intermetallic phase Co$_7$W$_6$ as previously for binary Co—W alloy [32], additional reflections of the intermetallic compound Co$_7$Mo$_6$, and rather wide halo with width about 15° is detected at angles 2θ of 43–58° (**Figure 6**) that reflects amorphous structure for both coatings deposited at pulse and direct current. The most important fact is the appearance of reflexes of metallic molybdenum and tungsten on XRD patterns for Co—Mo—W alloys deposited at pulse current. Such a character of X-ray diffraction patterns for coatings obtained by pulse current confirms our proposed mechanism of alloy formation [14, 28]. Metallic tungsten and molybdenum are formed in the chemical stage of reduction of refractory metal intermediate oxides during the pause of polarization. Such a pattern, along with decreasing tungsten content in the ternary alloy Co—Mo—W compared with a binary Co—W [32], also indicates molybdenum and tungsten competition during deposition in the alloy. The coherent-scattering region size of the amorphous part is 2–8 nm.
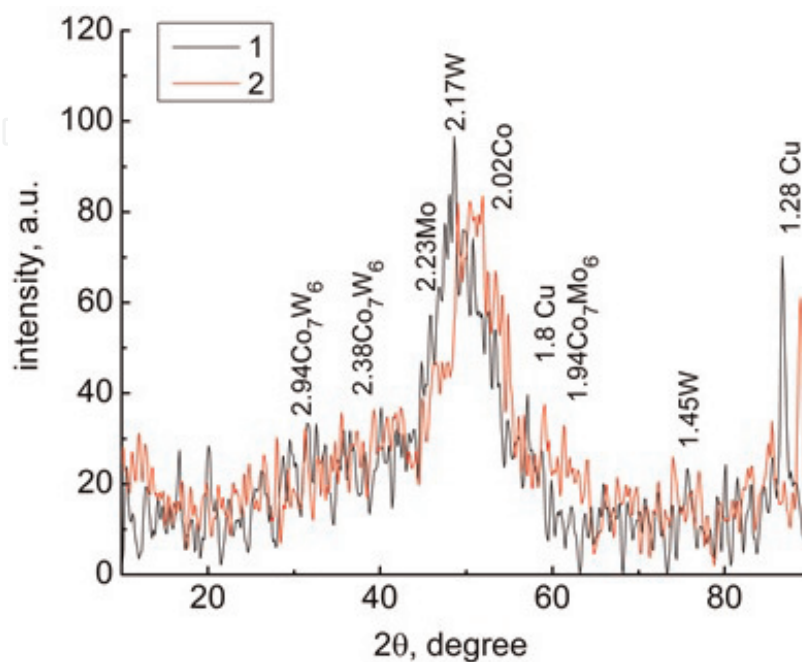
Figure 6.
X-ray diffraction patterns for electrolytic alloys Co—Mo—W of composition, at. %: (1) Co—75, Mo—16, W—9; (2) Co—85, Mo—9, W—5.

3. Co—Mo—Zr electrolytic alloys

The molybdenum content in Co—Mo—Zr alloys changes with current density increasing in the range of 2–4 A dm^{-2} (**Figure 7a**) similar to the Co—Mo—W films. At the same time, we observe a wider range of current densities of 4–8 A dm^{-2} providing coatings with molybdenum content of 24–25 at. %. Coating enrichment by molybdenum with increasing current density is entirely predictable since the molybdate electrochemical behavior is associated with multi-stage process following by chemical reducing of intermediate molybdenum oxides with hydrogen ad-atoms H$_{ad}$ [27, 29, 35]. The cathode potential at Co—Mo—Zr electrodeposition is rather negative $-(2.0$–$2.8)$ V (**Figure 7b**) and it becomes more negative with current density, that resulting in acceleration of side reaction producing H$_{ad}$ which are involved in a chemical step of reducing intermediate molybdenum oxides. Exactly due to above reasons, the molybdenum content in the deposits is increased. However, at current densities above 8 A dm^{-2}, hydrogen evolution reaction becomes the dominant as evidenced by the decreasing current efficiency (**Figure 7b**), whereby the molybdenum content in the alloy decreases.

The zirconium content in the ternary coatings reaches 3.6–3.7 at. % with increasing current density up to 4 A dm^{-2} (**Figure 7a**). As it follows from the experimental data as well as previous investigations [26], molybdenum and zirconium competition is observed when codeposited to get the ternary alloy at higher current density than of 4 A dm^{-2}. Such behavior is associated with the different mechanisms of alloying metals reducing from citrate-pyrophosphate electrolyte. Really, molybdate reducing to metallic state proceeds through the six electrons transfer accompanied by the removal of four oxygen atoms. Therefore, deposits may also contain incompletely reduced intermediate molybdenum oxides. Zirconium is likely included in the deposit in the form of oxygen compounds ZrO$_x$ due to higher binding energy Zr–O [31]. The EDS analysis data confirm the oxygen availability in the composition of the surface layers [31].

Nonlinear dependences of current efficiency Ce on the deposition current density (**Figure 7b**) were obtained, and Ce increases by 20% and reaches 63% with a rising current density from 5 to 8 A dm^{-2}; however, further increase in i reduces the current efficiency up to 47%. Such behavior may be attributed with acceleration of site hydrogen evolution reaction at more negative potentials.

Pulsed electrolysis allows the use of higher current densities, and not only energy parameter but also polarization time t_{on} and current interruption time t_{off} as well as its ratio are effectively used to control deposit composition and current efficiency. The shortest pulse duration should ensure the achievement of the alloy
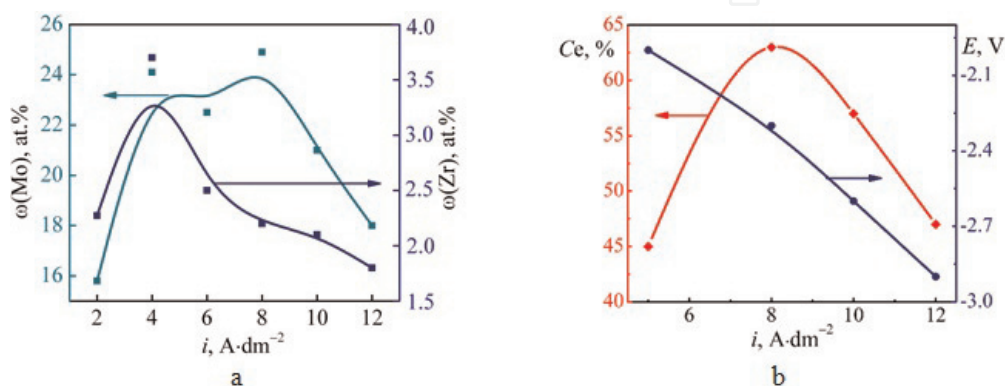
Figure 7.
Pulse current density influence on the composition (a) and current efficiency (b) for Co—Mo—Zr coatings; t_{on}/t_{off} 2/10 ms; T 20–25°C; pH 8; plated time 30 min.

deposition potential, as well as t_{on} is limited by the requirements for the visual quality of coatings and efficiency of electrolysis while minimizing side reactions.

Electrodeposition of Co—Mo—Zr alloys is the relevant example to demonstrate the benefits and flexibility of pulsed electrolysis control. Molybdenum and zirconium content in the alloys deposited at a current density of 4 A dm^{-2} rises when increasing pulse time of 0.5–2 ms while maintaining pause time 10 ms (**Figure 8a**). Obviously, the real current value increases at the expense of a full signal handling, thereby achieving potential of alloying metal reduction in alloy. However, an increase in the pulse duration of more than 2 ms reduces the zirconium content; therefore, it does not seem appropriate.

As follows from the experimental data (**Figure 8b**) prolong current interruption time of 5–10 ms everything else being equal promotes zirconium content in the alloy of 2.1 up to 3.7 at. %; although increasing the pause reduces the incorporation of this metal in the alloy. Thus, the top zirconium content in the electrolytic deposits is reached at the ratio t_{on}/t_{off} = 2/10 ms (duty factor q = 10 and f = 85 Hz). It should be stated, the molybdenum percentage in Co—Mo—Zr deposits rises from 16.0 to 24.0 at. % with the pause duration (**Figure 8b**) due to more complete chemical reducing of intermediate molybdenum oxides by H_{ad}. It also confirms difference in zirconium and molybdenum reducing mechanism as well as their competition when deposited into the alloy.

As for Co—Mo—W alloy, current efficiency of Co—Mo—Zr deposition decreases with increasing pulse time due to acceleration of side reaction. Prolonging the pause contributes to the current efficiency as the following chemical reactions accompanying the alloying metal discharge are more full; and a larger current interruption reduces the efficiency of the process. Thus, current efficiency reaches maximum 98% when t_{off} = 50 ms and t_{on} = 2 ms.

Surface morphology of Co—Mo—Zr coatings changes with increasing the current density amplified internal stress that leads to fracture grid (**Figure 9**). The coating surface becomes less smooth and more globular, and the crystallite sizes increase at the higher polarization and respectively at larger molybdenum content (**Figure 9a** and **c**). EDS analysis data (**Figure 10**) show sufficiently uniform distribution of the alloying metals on uneven relief of the deposits which is typical for pulsed electrolysis and emphasizes its advantage over stationary. Increasing in polarization time at a fixed pause contributes growth of irregular spheroids on the surface; and microcracks become larger as observed in [36]. Furthermore, the coatings deposited at the current density of 6–8 A dm^{-2} and on-time of 10 ms are more porous as compared with other (**Figure 9b** and **c**), apparently due to accelerated hydrogen evolution.
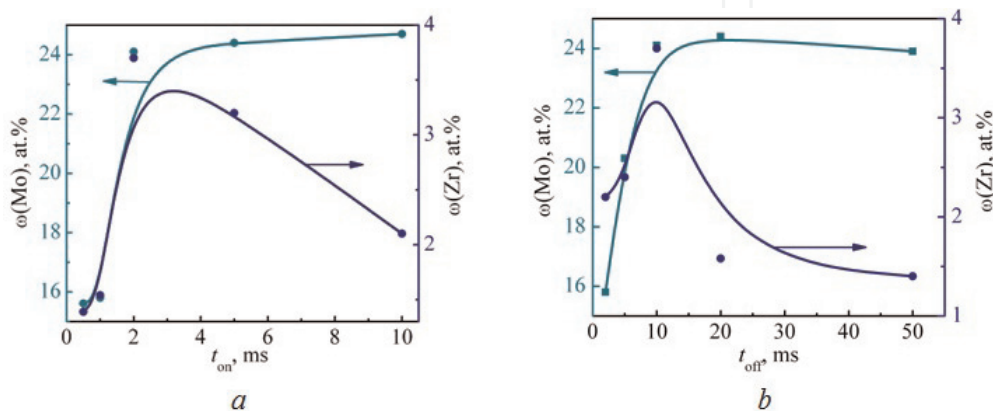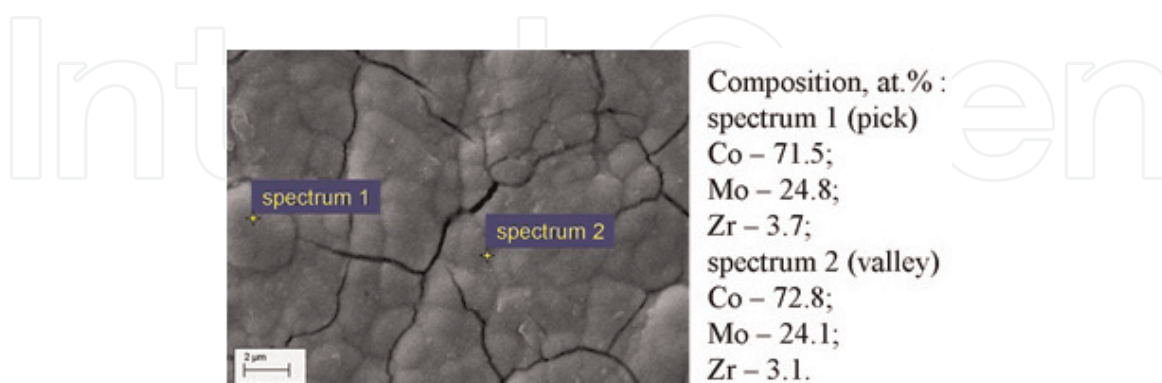

Figure 8.
Dependence of Co—Mo—Zr coating composition on the time of pulse t_{on} (a) (t_{off} 10 ms) and pause t_{off} (b) (t_{on} 2 ms); i = 4 A dm^{-2}; T = 20–25°C; pH 8; plated time 30 min.
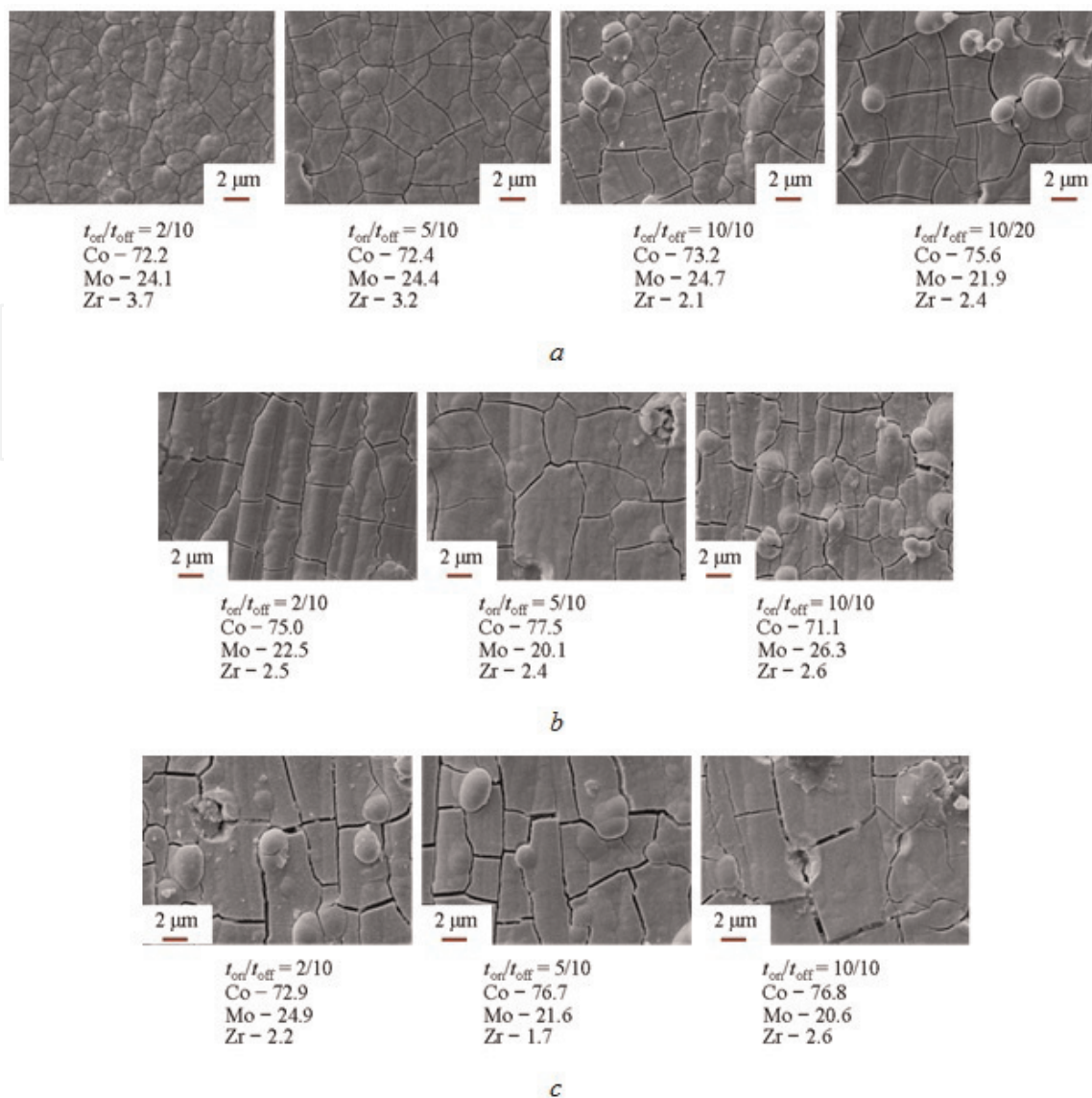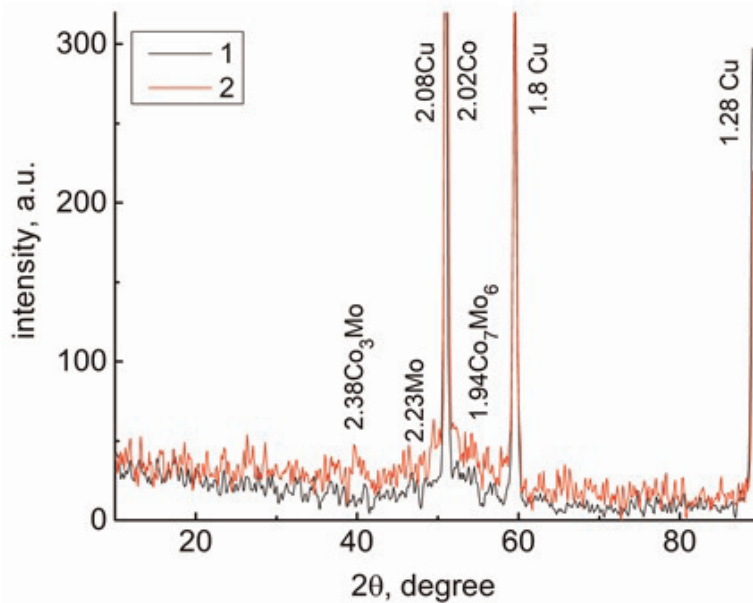
Figure 9.
Morphology (×2000) and composition (at. %) of Co—Mo—Zr coatings deposited in pulse mode at current density, A dm^{-2}: 4 (a); 6 (b) and 8 (c); T = 20–25°C; pH 8; plated time 30 min.

Figure 10.
Distribution of alloying elements at picks and valleys of coating Co—Mo—Zr deposited at 4 A dm^{-2}, t_{on}/t_{off} = 2/10.

Figure 11 shows X-ray diffraction patterns for electrolytic alloys Co—Mo—Zr deposited at a pulse current amplitude of 4 A dm^{-2} (**Figure 11** black line) and 8 A dm^{-2} (**Figure 11** red line). A series of diffraction lines for α-Co on X-ray diffraction patterns for Co—Mo—Zr deposits on steel substrates was obtained (**Figure 11**). The high intensity peaks at 52, 60, and 90° are copper substrate lines.

Figure 11.
X-ray diffraction patterns for electrolytic alloys Co━Mo━Zr of composition, at. %: (1) Co—72.2, Mo—24.1, Zr—3.7; (2) 72.9, Mo—24.9, Zr—2.2.

We can see peaks corresponding to intermetallic compounds Co_3Mo and Co_7Mo_6. Furthermore, one can find a small halo with full width at half maximum about 10° at angles 2θ 48–58° ~59°, which indicates an XRD amorphous structure of above materials [34]. Thus, the X-ray diffraction patterns indicate an amorphous-crystalline structure of the alloys. The most important fact is the appearance of reflexes of metallic molybdenum on XRD patterns for Co━Mo━Zr alloys deposited at higher current density 8 A dm^{-2} (**Figure 11** red line). In addition, the higher intensity of intermetallic compound reflexes is due to the enrichment of the alloy with the refractory component. The coherent-scattering region size of the amorphous part is 2–6 nm.

4. Corrosion behavior of binary and ternary cobalt electrolytic alloys

It is obvious that hydrogen ions H$^+$ are the oxidizing agents for cobalt-based electrolytic coatings in acidic medium, as well as in neutral and alkaline environment, only oxygen is a strong oxidizing agent [37]. Open circuit (corrosion) potentials E_{oc} of coated samples in corrosive solution with pH 3 are more positive than the potential of steel substrate which indicates the anodic control of corrosion process. The deep corrosion index k_h is reduced by almost three orders of magnitude (**Table 2**) and such inhibition in alloy corrosion is due to the acidic nature of refractory metals and zirconia oxides forming on the surface in oxygen containing media. The corrosion index of ternary alloys in acidic and neutral chloride-containing environment is almost halved compared with binary systems (**Table 2**). Such corrosion performance is associated with a decrease in roughness and smoothing out the relief of ternary coatings as compared with binary. In addition, the combined presence of molybdenum and tungsten or zirconium in the coatings provides a synergistic effect due to molybdenum and tungsten enhancing corrosion resistance to pitting as well as zirconium increasing tend to passivity. Moreover, with increasing total content of alloying metals, corrosion resistance increases.

Open circuit potentials of coated samples in corrosive solution with pH 11 are slow negative as compared with steel substrate (**Table 2**), that stipulates cathodic

Electrolytic alloy composition, at. %	Corrosive medium based on 1 M Na$_2$SO$_4$					
	pH 3		3% NaCl (pH 7)		pH 11	
	E_{oc}, V	k_h, mm/year	E_{oc}, V	k_h, mm/year	E_{oc}, V	k_h, mm/year
Steel substrate	−0.62	1.85	−0.56	0.93	−0.43	0.12
Co$_{76}$—Mo$_{24}$	−0.42	0.023	−0.25	0.029	−0.43	0.003
Co$_{84}$—W$_{16}$	−0.32	0.024	−0.35	0.01	−0.44	0.004
Co$_{83}$—Mo$_{12}$—W$_5$	−0.22	0.012	−0.37	0.007	−0.47	0.008
Co$_{79}$—Mo$_{16}$—W$_5$	−0.25	0.012	−0.38	0.005	−0.50	0.007
Co$_{72}$—Mo$_{24}$—Zr$_4$	−0.46	0.003	−0.5	0.002	−0.47	0.003
Co$_{73}$—Mo$_{25}$—Zr$_2$	−0.47	0.004	−0.5	0.003	−0.48	0.005

Table 2.
Corrosion indicators (E_{oc}, V; k_h, mm per year) of testing materials in different media.

Electrolytic alloy composition, at. %		Functional properties	Application area	Reference
Co	45–80	Hv 450–1100 MN/m^2	High hard, wear, heat resistant	[12, 15, 32]
Mo	14–34	lgi^0_H (Co$_{71}$Mo$_{16}$W$_{13}$) = −3.35	and corrosion protective coatings	
W	5–15	[A/cm^2]		
Co	70–80	Hv 450–900 MN/m^2	Corrosion protective coatings,	[26, 31]
Mo	15–25	lgi^0_H (Co$_{75}$Mo$_{21}$Zr$_4$) = −3.1	electrocatalytic films	
Zr	2–4	[A cm^2]		

Table 3.
Application areas for the cobalt ternary coatings.

control of corrosion process. Such corrosion performance is mainly due to the basic nature of cobalt (II) oxides and hydroxides, which hinders the oxygen transport. The difference in corrosion rate of substrate and coated samples in such conditions is somewhat less—the deep corrosion index k_h is reduced by almost two orders of magnitude.

Summarizing and relying on the results of earlier studies [12, 15, 26, 31, 32] of the ternary cobalt alloy functional properties, it is possible to present their application areas in the table form (**Table 3**). This table reflects the composition, appropriative properties (microhardness Hv, corrosion resistance, and catalytic activity in hydrogen evolution reaction indicated as hydrogen exchange current density lgi^0_H), and technological application of designed coatings.

5. Summarizing the observations

Ternary Co—Mo—W electrolytic alloys deposited from citrate-pyrophosphate bath at pulse current composition and surface morphology were shown to be dependent on the current density and on/off time. The top refractory metal content in deposits was obtained at the current density of 9–10 A dm^{-2} and on/off time of 5/20 ms, but increasing current density diminishes efficiency of electrolysis. Tungsten content in the alloy was found to be much lower than molybdenum: W—2–7 at. % *vs*

Mo—16–22 at. % when depositing Co—Mo—W from the electrolyte with the oxometalate ratio Mo:W as 1:2. Structure of the ternary alloys was found to be amorphous-crystalline, and coherent-scattering region size was detected of 2–8 nm. Ternary coatings contain intermetallic phases Co_7W_6 and Co_7Mo_3. The amorphous structure of ternary alloys and significant content of alloying elements (Mo and W) provide high corrosion resistance increasing with total content of refractory metals.

Ternary galvanic alloys Co—Mo—Zr of different compositions and morphologies are deposited from citrate-pyrophosphate electrolyte at pulse current. Coatings with micro-globular morphology possessing low level of stress and cracks are formed at the current density of 4–6 A dm^{-2} and on/off time 2/10 ms. Structure of Co—Mo—Zr alloys was found to be amorphous crystalline, and coherent-scattering region size was detected of 2–6 nm. Ternary coatings contain intermetallic phases Co_3Mo and Co_7Mo_6. Co—Mo—Zr coatings high corrosion resistance is due to the molybdenum and zirconium tend to passivity, as well as the acid nature of their oxides.

The designed coating application areas corresponding to the functional properties are presented.

Author details

Gulmira Yar-Mukhamedova[1*], Maryna Ved'[2], Nikolay Sakhnenko[2] and Tetiana Nenastina[2]

1 Institute of Experimental and Theoretical Physics of Al-Farabi Kazakh National University, Almaty, Kazakhstan

2 National Technical University "Kharkiv Polytechnic Institute", Kharkiv, Ukraine

*Address all correspondence to: gulmira-alma-ata@mail.ru

IntechOpen

References

[1] Alexandrov Y, Pospelow A, Ved' M, et al. New application of electrode impedance spectroscopy in electrosynthesis of the organic conductors. In: Abstracts of NATO ARW "Recent Advances towards New Technologies"; 14-18 September 2003; Sudak, Crimea, Ukraine. 2003. p. 52

[2] Alexandrov Y, Sakhnenko N, Pospelow A, et al. Ion-selective electrodes based on organic conductors. In: Abstracts of the 5-th Int. Conf. "Electronic Processes in Organic Materials" (ICEPOM-5); 24-29 May 2004; Kyiv: Naukoviy Svit. 2004. pp. 209-210

[3] Sakhnenko MD, Ved' MV, Bairachna TM. Electrolytic alloys: Origin of synergetic effects. In: Materials of Conference Applied physico-inorganic chemistry; Simferopol: DIP. 2013. p. 53

[4] Yar-Mukhamedova GS. Influence of thermal treatment on corrosion resistance of chromium and nickel composite coatings. Materials Science. 2000;**36**:922-924. DOI: 10.1023/A: 1011355325698

[5] Ved' M, Sakhnenko N, Bairachnaya T, Tkachenko N. Structure and properties of electrolytic cobalt-tungsten alloy coatings. Functional Materials. 2008;**15**:613-617

[6] Ahmad J, Asami K, Takeuchi A, Louzguine DV, Inoue A. High strength Ni-Fe-W and Ni-Fe-W-P alloys produced by electrodeposition. Materials Transactions. 2003;**44**(10): 1942-1947. Special issue on nano-hetero structures in advanced metallic materials

[7] Ved' MV, Sakhnenko ND, Karakurkchi AV, Zyubanova SI. Electrodeposition of iron-molybdenum coatings from citrate electrolyte. Russian Journal of Applied Chemistry.

2014;**87**:276-282. DOI: 10.1134/ S1070427214030057

[8] Yao S, Zhao S, Guo H, Kowaka M. A new amorphous alloy deposit with high corrosion resistance. Corrosion. 1996; **52**(3):183-186. DOI: 10.5006/1.3292112

[9] Tsyntsaru N, Cesiulis H, Donten M, Sort J, Pellicer E, Podlaha-Murphy EJ. Modern trends in tungsten alloys electrodeposition with iron group metals. Surface Engineering and Applied Electrochemistry. 2012;**48**: 491-520. DOI: 10.3103/ S1068375512060038

[10] Kohli S, Miglani S, Rapariya R. Basics of artificial neural network. International Journal of Computer Science and Mobile Computing. 2014;**3**: 745-751

[11] Ved' MV, Sakhnenko MD, Shtefan VV, et al. Computer modeling of the nonchromate treatment of aluminum alloys by neural networks. Materials Science. 2008;**44**(2):216-221

[12] Sakhnenko MD, Ved' MV, Ermolenko IY, Hapon YK, Kozyar MO. Design, synthesis, and diagnostics of functional galvanic coatings made of multicomponent alloys. Materials Science. 2017;**53**:680-686. DOI: 10.1007/ s11003-017-0009-7

[13] Yermolenko IY, Ved' MV, Sakhnenko ND, Sachanova YI. Composition, morphology, and topography of galvanic coatings Fe-Co-W and Fe-Co-Mo. Nanoscale Research Letters. 2017;**12**:352. DOI: 10.1186/ s11671-017-2128-3

[14] Karakurkchi AV, Ved' MV, Yermolenko IY, Sakhnenko ND. Electrochemical deposition of Fe–Mo–W alloy coatings from citrate electrolyte. Surface Engineering and

Applied Electrochemistry. 2016;**52**: 43-49. DOI: 10.3103/S1068375516010087

[15] Sakhnenko ND, Ved' MV, Hapon YK, Nenastina TA. Functional coatings of ternary alloys of cobalt with refractory metals. Russian Journal of Applied Chemistry. 2015;**87**:1941-1945. DOI: 10.1134/S107042721501206X

[16] Silkin SA, Gotelyak AV, Tsyntsaru N, Dikusar AI, Kreivaitis R, Padgurskas J. Effect of bulk current density on tribological properties of Fe-W, Co-W and Ni-W coatings. In: Proceedings of the 8th International Scientific Conference "BALTTRIB 2015". 2016. pp. 51-56. DOI: 10.15544/balttrib.2015.10

[17] Glushkova MA, Bairachna TN, Ved' MV, Sakhnenko ND. Electrodeposited cobalt alloys as materials for energy technology. In: Mater. Res. Soc. Symp. Proc.; USA, Boston. Vol. 1491. 2013. p. mrsf12-1491-c08-15. DOI: 10.1557/opl.2012.1672

[18] Ma SL, Xi X, Nie Z, Dong T, Mao Y. Electrodeposition and characterization of Co-W alloy from regenerated tungsten. International Journal of Electrochemical Science. 2017;**12**: 1034-1051. DOI: 10.20964/2017.02.37

[19] Capel H, Shipway PH, Harris SJ. Sliding wear behaviour of electrodeposited cobalt–tungsten and cobalt–tungsten–iron alloys. Wear. 2003;**255**:917-923. DOI: 10.1016/S0043-1648(03)00241-2

[20] Gomez E, Pellicer E, Alcobe X, Valles E. Properties of Co-Mo coatings obtained by electrodeposition at p. 6.6. Journal of Solid State Electrochemistry. 2004;**8**:497-504. DOI: 10.1007/s10008-004-0495-z

[21] Gomez E, Pellicer E, Valles E. Electrodeposited cobalt_molybdenum magnetic materials. Journal of Electroanalytical Chemistry. 2001;**517**:

109-116. DOI: 10.1016/S0022-0728(01)00682-9

[22] Gomez E, Kipervaser ZG, Pellicer E, Valles E. Extracting deposition parameters for cobalt–molybdenum alloy from potentiostatic current transients. Physical Chemistry Chemical Physics. 2004;**6**:1340-1344. DOI: 10.1039/B315057G

[23] Yar-Mukhamedova G, Ved' M, Sakhnenko N, Karakurkchi A, Yermolenko I. Iron binary and ternary coatings with molybdenum and tungsten. Applied Surface Science. 2016; **383**:346-352. DOI: 10.1016/j.apsusc.2016.04.046

[24] Karakurkchi AV, Ved' MV, Sakhnenko ND, Ermolenko IY. Electrodeposition of iron–molybdenum–tungsten coatings from citrate electrolytes. Russian Journal of Applied Chemistry. 2015;**88**:1860-1869. DOI: 10.1134/S107042721501108X

[25] Yermolenko IY, Ved' MV, Karakurkchi AV, Sakhnenko ND, Kolupayeva ZI. The electrochemical behavior of Fe^{3+}–WO_4^{2-}–Cit^{3-} and Fe^{3+}–MoO_4^{2-}–WO_4^{2-}–Cit^{3-} systems. Issues of Chemistry and Chemical Technology. 2017;**2**:4-14

[26] Yar-Mukhamedova G, Ved' M, Sakhnenko N, Koziar M. Ternary cobalt-molybdenum-zirconium coatings for alternative energies. Applied Surface Science. 2017;**421**(Part A):68-76. DOI: 10.1016/j.apsusc.2017.01.196

[27] Yar-Mukhamedova GS, Sakhnenko ND, Ved' MV, Yermolenko IY, Zyubanova SI. Surface analysis of Fe-Co-Mo electrolytic coatings. In: IOP Conference Series: Materials Science and Engineering. Vol. 213. 2017. DOI: 10.1088/1757-899X/213/1/012019

[28] Ved' MV, Ermolenko IY, Sakhnenko ND, Zyubanova SI, Sachanova YI. Methods for controlling the composition

and morphology of electrodeposited Fe–Mo and Fe–Co–Mo coatings. Surface Engineering and Applied Electrochemistry. 2017;**53**(6):525-532. DOI: 10.3103/S1068375517060138

[29] Shao II, Vereecken PM, Chien CL, Cammarata RC, Searson PC. Electrochemical deposition of FeCo and FeCoV alloys. Journal of the Electrochemical Society. 2003;**150**: C184-C188. DOI: 10.1149/1.1553789

[30] Ved' MV, Sakhnenko ND, Yermolenko IY, Nenastina TA. Nanostructured functional coatings of iron family metals with refractory elements. Chapter 1. In: Fesenko O, Yatsenko L, editors. Nanochemistry, Biotechnology, Nanomaterials, and Their Applications, Springer Proceedings in Physics. Vol. 214. Cham, Switzerland: Springer International Publishing AG, part of Springer Nature; 2018. pp. 3-34. DOI: 10.1007/978-3-319-92567-7_1

[31] Ved' M, Sakhnenko N, Koziar M, Slavkova M. Functional properties of electrolytic alloys of cobalt with molybdenum and zirconium. Functional Materials. 2016;**23**:420-426. DOI: 10.15407/fm23.03.420

[32] Yar-Mukhamedova G, Ved' M, Sakhnenko N, Nenastina T. Electrodeposition and properties of binary and ternary cobalt alloys with molybdenum and tungsten. Applied Surface Science. 2018;**445**:298-307. DOI: 10.1016/j.apsusc.2018.03.171

[33] Schlesinger M, Paunovic M. Modern Electroplating. 5th ed. Hoboken, NJ: John Wiley & Sons; 2010

[34] Ramanauskas R, Gudavičiūtė L, Juškėnas R. Effect of pulse plating on the composition and corrosion properties of Zn–Co and Zn–Fe alloy coatings. Chemija. 2008;**19**:7-13

[35] Tsyntsaru N, Cesiulis H, Budreika A. The effect of electrodeposition conditions and post-annealing on nanostructure of Co–W coatings. Surface and Coating Technology. 2012; **206**:4262-4269. DOI: 10.1016/j. surfcoat.2012.04.036

[36] Pustovalov EV, Modin EB, Voitenko OV, Fedorets AN, Dubinets AV, Grudin BN, et al. Structure relaxation and crystallization of the CoW-CoNiW-NiW electrodeposited alloys. Nanoscale Research Letters. 2014;**9**:66. DOI: 10.1186/1556-276X-9-66

[37] Tsyntsaru N, Dikusar A, Cesiulis H, Celis J-P, Bobanova Z, Sidel'nikova S, et al. Tribological and corrosive characteristics of electrochemical coatings based on cobalt and iron superalloys. Powder Metallurgy and Metal Ceramics. 2009;**48**:419-428. DOI: 10.1007/s11106-009-9150-7